Interaction of ultrashort laser pulses with metal surfaces: Impulsive jellium-Volkov approximation versus the solution of the time-dependent Schrödinger equation

M. N. Faraggi,[1,2] M. S. Gravielle,[1,2] and D. M. Mitnik[1,2]
[1]*Instituto de Astronomía y Física del Espacio, CONICET, Casilla de Correo 67, Sucursal 28, 1428 Buenos Aires, Argentina*
[2]*Departamento de Física, FCEN, Universidad de Buenos Aires, Buenos Aires, Argentina*
(Received 26 March 2007; published 25 July 2007)

Electron emission coming from the valence band of metal surfaces due to grazing incidence of high-frequency ultrashort laser pulses is studied. We introduce a distorted-wave method, named impulsive jellium-Volkov (IJV) approximation, in which the surface is represented by the jellium model while the interaction with the laser field is described by means of the Volkov phase. With the purpose of examining the proposed approach, we compare IJV results with values derived from the numerical solution of the corresponding time-dependent Schrödinger equation (TDSE). For Al(111) surfaces, double and single differential probability spectra are calculated considering different durations of the laser pulse. Very good agreement between IJV and TDSE results was found. The total probability dependence on the intensity and carrier-envelope phase of the pulse is also investigated.

DOI: 10.1103/PhysRevA.76.012903 PACS number(s): 34.50.Dy, 34.50.Bw

I. INTRODUCTION

In recent years, research on electromagnetic pulses interacting with matter has been widely developed not only in the theoretical area [1,2] but also in the experimental one [3,4]. In particular, the photoelectron emission produced by the action of strong laser fields on solid surfaces has opened the way to understanding several nonlinear processes [5–7].

The present paper deals with electron emission from metal surfaces induced by grazing incidence of ultrashort laser pulses. Our aim is to derive a simple approximation, within the time-dependent distorted-wave formalism, which takes into account the main features of the process. For this purpose we introduce the impulsive jellium-Volkov (IJV) approximation, which combines a simple representation of the surface interaction—given by the jellium model—with the Volkov wave function, which describes the action of the electromagnetic field on the emitted electron [8]. Unlike the surface-Volkov (SV) approach, developed in a previous paper [9], the IJV theory includes the complete Volkov phase, containing the space shift of the final state produced by the external field.

In the jellium model, electrons of the valence band are bound to the surface by a finite step potential, and the corresponding electronic states are represented by analytical expressions that include the proper asymptotic conditions [10]. Even though the jellium model does not contain any information about the band structure of the solid, it has proved to give an adequate description of the electron-surface interaction in grazing ion-surface collisions [11].

To analyze the validity of the proposed approximation, we compare IJV results with values obtained by solving numerically the time-dependent Schrödinger equation (TDSE) corresponding to the jellium potential for a slab. Both methods, the IJV approach and the numerical solution of the TDSE are applied to evaluate photoelectron emission from the valence band of Al (111) produced by intense and few-cycle laser pulses, with high carrier frequencies.

The momentum distributions of the emitted electrons are studied for different durations of the pulse, allowing from zero to several oscillations of the electric field. We also investigate the dependence of the total emission probability on the intensity and the carrier-envelope phase of the laser pulse. The paper has been organized as follows. Theory is presented in Sec. II, results are shown and discussed in Sec. III, and conclusions are summarized in Sec. IV. Atomic units are used throughout unless otherwise stated.

II. THEORY

When a laser pulse impinges at grazing incidence on a metal surface (S), an electron (e) of the valence band of the solid, initially in the state i, can be ejected to the vacuum zone, ending in the final state f. The frame of reference is placed at the position of the crystal border, with the $\hat{z}$ axis in the direction perpendicular to the surface, aiming toward the vacuum region.

We consider a laser pulse associated with a linearly polarized electric field $\mathbf{F}(t)$. According to the grazing incidence condition, the field $\mathbf{F}(t)$ is oriented perpendicular to the surface, along the $\hat{z}$ axis. The temporal profile of the pulse is defined as

$$F(t) = F_0 \sin(\omega t + \varphi)\sin^2(\pi t/\tau) \tag{1}$$

for $0 < t < \tau$, and 0 elsewhere, where F_0 is the maximum field strength, ω is the carrier frequency, φ represents the carrier-envelope phase, and τ determines the duration of the pulse.

The frequency of the laser pulse is here restricted to the range $\omega > \omega_s$, with ω_s the surface plasmon frequency. For such a high frequency, the induced surface potential, which is associated with the response of the surface to the external field, is much smaller than the laser interaction, and its effect on the emitted electron can be neglected. Under this assumption, the temporal evolution of the electronic state $\Psi(\mathbf{r},t)$ is determined by the time-dependent Schrödinger equation

$$i\frac{\partial\Psi(\mathbf{r},t)}{\partial t} = [H_0 + V_L(z,t)]\Psi(\mathbf{r},t), \tag{2}$$

where $\mathbf{r}\equiv(\mathbf{r}_s,z)$ is the position vector of the active electron e, with $\mathbf{r}_s$ and z the components parallel and perpendicular to the surface, respectively. In Eq. (2), $H_0=-\nabla_{\mathbf{r}}^2/2+V_S$ is the unperturbed Hamiltonian associated with the electron bound to the surface, with V_S the electron-surface potential, and $V_L(z,t)=zF(t)$ is the interaction potential with the laser field, expressed in the length gauge.

To describe the metal surface, we use the jellium model, in which V_S is represented by a step potential $V_S=-V_c\Theta(-z)$, with $V_c=E_F+E_W$, where E_F is the Fermi energy, E_W is the work function, and Θ denotes the unitary Heaviside function. Within the jellium model, the eigenfunctions of H_0 with momentum $\mathbf{k}=(\mathbf{k}_s,k_z)$, measured inside the solid, and energy $E_{\mathbf{k}}=k_s^2/2+\epsilon_{k_z}$ are expressed as

$$\Phi_{\mathbf{k}}^{\pm}(\mathbf{r},t) = \frac{e^{i\mathbf{k}_s\cdot\mathbf{r}_s}}{2\pi}\phi_{k_z}^{\pm}(z)e^{-iE_{\mathbf{k}}t}, \tag{3}$$

where the $\pm$ signs indicate the outgoing $(+)$ and incoming $(-)$ asymptotic conditions. The functions $\phi_{k_z}^{\pm}(z)$ represent the eigenfunctions with eigenenergy ϵ_{k_z} corresponding to the one-dimensional potential V_S. Explicit expressions for them are given in the Appendix of Ref. [10].

The differential probability of electron emission from the surface is expressed in terms of the transition matrix as

$$\frac{dP}{d\mathbf{k}_f'} = \rho_e\frac{k_{fz}'}{k_{fz}}\int d\mathbf{k}_i\Theta(v_F-k_i)|T_{if}|^2, \tag{4}$$

where T_{if} is the T-matrix element corresponding to the inelastic transition $\mathbf{k}_i\rightarrow\mathbf{k}_f'$ and $\mathbf{k}_f'=(\mathbf{k}_{fs},k_{fz}')$ is the final electron momentum outside the solid, with $k_{fz}'=(k_{fz}^2-2V_c)^{1/2}$. In Eq. (4), $\rho_e=2$ takes into account the spin states and Θ restricts the initial states to those contained inside the Fermi sphere, with $v_F=(2E_F)^{1/2}$.

In this work we evaluate T_{if} by employing two different methods: the IJV approximation and the numerical solution of the TDSE. Both of them are summarized below.

A. Impulsive jellium-Volkov approximation

Within the time-dependent distorted-wave formalism, it is possible to derive an approximate solution of Eq. (2) by using the well-known impulsive approach [12]. Under this hypothesis the electronic state for the final channel can be represented by the impulse jellium-Volkov wave function, which is built from the unperturbed state by including the action of the laser field by means of the phase of the Volkov state [8,13]. The Volkov wave function represents the exact solution for a free electron moving in a time-dependent electric field and has been successfully used to describe atomic processes [14–16]. The final IJV wave function reads

$$\chi_f^{(IJV)-}(\mathbf{r},t) = \Phi_{\mathbf{k}_f}^{-}(\mathbf{r},t)\exp[iD^-(k_{fz},z,t)], \tag{5}$$

where

$$D^-(k_{fz},z,t) = \frac{z}{c}A^-(t) - \beta^-(t) - k_{fz}\alpha^-(t) \tag{6}$$

is the Volkov phase, and $\Phi_{\mathbf{k}_f}^-$ is the final unperturbed state-given by Eq. (3)—with $\phi_{k_z}^-$ corresponding to the external ionization process, associated with electrons ejected toward the vacuum zone. The functions involved in Eq. (6),

$$A^-(t) = -c\int_{+\infty}^{t} dt' F(t'),$$

$$\beta^-(t) = (2c^2)^{-1}\int_{+\infty}^{t} dt'[A^-(t')]^2,$$

$$\alpha^-(t) = c^{-1}\int_{+\infty}^{t} dt' A^-(t'), \tag{7}$$

are related to the vector potential, the ponderomotive energy, and the quiver amplitude, respectively, with c the light velocity.

By employing the IJV and unperturbed wave functions in the final and initial channels, respectively, the distorted-wave transition amplitude [17] reads

$$T_{if}^{(IJV)} = a_{fi} - i\int_{-\infty}^{+\infty} dt\langle\chi_f^{(IJV)-}(t)|W_f^{\dagger}(t)|\Phi_{\mathbf{k}_i}^{+}(t)\rangle$$

$$= -i\int_{-\infty}^{+\infty} dt\langle\chi_f^{(IJV)-}(t)|V_L(z,t)|\Phi_{\mathbf{k}_i}^{+}(t)\rangle, \tag{8}$$

where

$$a_{fi} = \lim_{t\rightarrow-\infty}\langle\chi_f^{(IJV)-}(t)|\Phi_{\mathbf{k}_i}^{+}(t)\rangle \tag{9}$$

is the sudden transition amplitude, corresponding to a simple step process, and $W_f(t)$ denotes the final distortion potential, which is derived from $W_f(t)|\chi_f^{(IJV)-}(t)\rangle=[H_0+V_L(z,t)-id/dt]|\chi_f^{(IJV)-}(t)\rangle$. After some algebra, $T_{if}^{(IJV)}$ reads

$$T_{if}^{(IJV)} = -i\delta(\mathbf{k}_{fs}-\mathbf{k}_{is})\int_0^{\tau} dt\, F(t)G_{if}(t)\exp[i\Delta\epsilon t + i\beta^-(t)], \tag{10}$$

where the δ function expresses the momentum conservation in the direction parallel to the surface and $\Delta\epsilon=\epsilon_{k_{fz}}-\epsilon_{k_{iz}}$ is the perpendicular energy gained during the transition. The function G_{if} is defined as

$$G_{if}(t) = \int_{-\infty}^{+\infty} dz\ \phi_{k_{fz}}^{-*}(\tilde{z})z\exp[iQ_z(t)z]\phi_{k_{iz}}^{+}(z), \tag{11}$$

where $Q_z(t)=-A^-(t)/c$ represents the momentum transferred by the field and $\tilde{z}$ denotes the coordinate z shifted by the quiver amplitude, i.e., $\tilde{z}=z-\alpha^-(t)$. Note that for the jellium model G_{if} displays a closed form.

B. TDSE solution

The T-matrix element involved in Eq. (4) can also be obtained by propagating the TDSE given by Eq. (2) in a

numerical lattice. The problem is reduced to a one-dimensional equation by employing the parallel invariance of the surface and laser interactions, which allows us to express the electronic state as

$$\Psi_{\mathbf{k}}(\mathbf{r},t) = \frac{e^{i\mathbf{k}_s\cdot\mathbf{r}_s}}{2\pi}\Psi_{k_z}(z,t)e^{(-ik_s^2t)/2}. \quad (12)$$

In order to find a numerical solution for $\Psi_{k_z}(z,t)$, we first replace the jellium potential V_S by a smoothed well potential $\mathcal{V}_S$ of depth V_c and width L. Then we solve the time-independent Schrödinger equation

$$h_0\varphi_{k_z}(z) = \epsilon_{k_z}\varphi_{k_z}(z) \quad (13)$$

by diagonalizing the one-dimensional unperturbed Hamiltonian $h_0(z)=-(1/2)d^2/dz^2+\mathcal{V}_S(z)$.

Every initial bound eigenfunction $\varphi_{k_{iz}}(z)$ is propagated through the TDSE associated with the Hamiltonian $h(z,t)=h_0(z)+V_L(z,t)$ and their respective solutions are

$$\Psi_{k_{iz}}(z,t) = \exp\left(-i\int_0^t h(z,t)dt\right)\varphi_{k_{iz}}(z). \quad (14)$$

The time evolution is performed by using an explicit leap-frog time propagator [18]. This method involves only one Hamiltonian matrix multiplication per time step and it is easily implemented on massively parallel computers. Unitarity is satisfied provided the time step is smaller than the inverse of the largest Hamiltonian eigenvalue. This method has proved very suitable for many calculations of electron-impact ionization and photoionization of atoms (see Refs. [19,20] for a review).

After a time t_f slightly longer than the pulse duration, i.e., $t_f > \tau$, the evolved wave function is used to calculate the ionization amplitude by projecting it on to every particular final continuum state $\varphi_{k_{fz}}(z)$. Then the TDSE transition amplitude can be expressed in terms of the z amplitude as

$$T_{if}^{(TDSE)} = \delta(\mathbf{k}_{fs}-\mathbf{k}_{is})\langle\varphi_{k_{fz}}(z)|\Psi_{k_{iz}}(z,t_f)\rangle. \quad (15)$$

III. RESULTS

We apply the proposed models to evaluate electron emission from Al(111), which is here considered as a benchmark for the theory. The parameters that characterize the Al(111) surface are the Fermi energy $E_F=0.414$ a.u., the work function $E_W=0.156$ a.u., and the surface plasmon frequency $\omega_s=0.40$ a.u. We consider laser pulses with field strengths up to $F_0=0.1$ a.u., which, albeit intense, belong to the perturbative regime, far from the saturation region. Because the induced surface potential is not taken into account in the formalism, carrier frequencies ω are limited to values larger than the plasmon frequency ω_s. In all the cases, except in Fig. 6 where the dependence on the carrier-envelope phase is analyzed, we employ symmetric pulses, with $\varphi=-\omega\tau/2+\pi/2$.

In the calculation of $T_{if}^{(IJV)}$, the numerical integration on the time involved in Eq. (10) was obtained with an error of 1%. For the evaluation of the TDSE solution we used a numerical lattice of 800 a.u. spanned by a uniform mesh with spacing $\Delta z=0.1$ a.u. The well potential $\mathcal{V}_S$ was chosen with a width $L=400$ a.u. Under these conditions, Eq. (13) results in 138 bound levels and 508 continuum states in the range $0\leqslant\epsilon_{k_z}\leqslant 2.9$ a.u. The time propagation of Eq. (14) was performed with a time step $\Delta t=4.05\times10^{-4}$ a.u. In both IJV and TDSE methods, the parallel momentum conservation, imposed by the δ function in Eqs. (10) and (15) respectively, reduces the integration on the initial momentum involved in Eq. (4) to a one-dimensional integral on k_{iz}. This further integration was solved by interpolating up to 100 points in the case of the IJV approach, and by adding over all the initial occupied states in the TDSE method.

It is important to note that the final states employed in the IJV approximation contain the proper asymptotic conditions, while those derived from the numerical solution of Eq. (13) do not allow us to distinguish electrons emitted toward the bulk from those expelled outside the solid. Then, as a first estimation, within the TDSE method we averaged the contributions coming from final states with near energies, weighting them with the fraction of electrons emitted toward the vacuum that is derived from the IJV model.

A. Electron distributions

The proposed distorted-wave method is analyzed by comparing IJV results with values obtained from the numerical solution of the TDSE. The goal is to determine the grade of accuracy of IJV predictions to describe a simplified scenario of the interaction of strong ultrashort laser pulses with surfaces, as given by the jellium model.

First, we study the angular distribution of emitted electrons, which is derived from Eq. (4) as $d^2P/dE_fd\Omega_f=k_f'dP/d\mathbf{k}_f'$, where E_f and Ω_f are the final energy and solid angle, respectively, of the ejected electron and $k_f'=|\mathbf{k}_f'|$. In Fig. 1 we show electron distributions for laser pulses with $F_0=0.1$ a.u., $\omega=1$ a.u., and duration times (a) $\tau=4$ a.u. and (b) $\tau=40$ a.u. In both cases, IJV probabilities for different emission angles θ_e, measured with respect to the surface, are displayed. As a consequence of the geometry of the problem, the maximum emission probability corresponds to the angle $\theta_e=90^\circ$, which coincides with the direction of the laser field. Therefore, for this particular orientation of emitted electrons we also plot TDSE values of $d^2P/dE_fd\Omega_f$.

For $\tau=4$ a.u. [Fig. 1(a)], the pulse does not display any oscillation inside the envelope, corresponding to the so-called collisional regime because of the similarities between the electromagnetic potential associated with $\mathbf{F}(t)$ and the one produced by a swift grazing projectile. We find that for this ultrashort pulse, IJV and TDSE probabilities are similar in the whole electron energy range, decreasing smoothly as the electron velocity increases.

For a longer pulse, as considered in Fig. 1(b), the field performs several oscillations inside the envelope. Then the electron spectrum displays the characteristic pattern of the multiphoton mechanism, with peaks spaced out the photon energy ω. For this pulse, IJV predictions for $\theta_e=90^\circ$ agree again with the TDSE data, overestimating these last values only slightly around the second maximum.

Note that, in spite of the general agreement observed between the two theories, IJV double differential probabilities

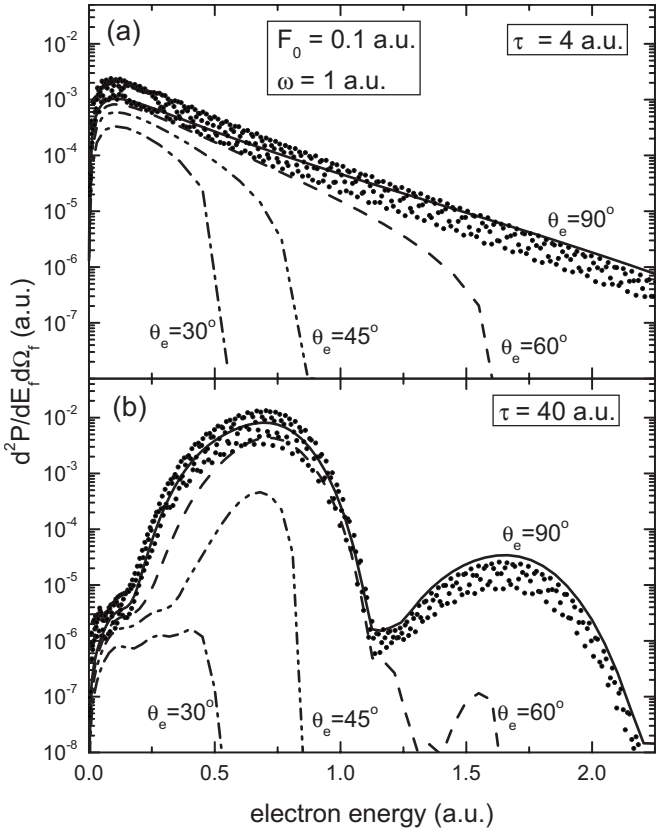

FIG. 1. Differential electron emission probability as a function of the electron energy. The parameters of the laser field are F_0 =0.1 a.u., ω=1 a.u., and τ=(a) 4 and (b) 40 a.u. Lines, IJV results for different ejection angles θ_e; full dots, TDSE data for θ_e=90°.

lie on a smooth curve while the TDSE values present a quite wide spread, which could be associated with the use of a discrete grid. In all cases, the maximum energy that the ejected electron can reach depends on the emission angle, decreasing when θ_e diminishes. This effect is due to the conservation of the parallel momentum, imposed by the δ function in Eqs. (10) and (15), which is combined with the restriction of keeping the initial electron momentum inside the Fermi sphere.

By comparing Fig. 1 with the corresponding one of Ref. [9] we observe that, even though the IJV theory shows a qualitatively similar behavior to the SV approach, the inclusion of the quiver amplitude, neglected in the SV theory, introduces substantial changes in the electron spectra, especially at high electron energies.

Differential probabilities of electron emission in the direction perpendicular to the surface are plotted in Fig. 2 for a laser field with a lower strength, F_0=0.05 a.u., and a duration of τ=40 a.u. For the two different carrier frequencies—ω=1 and 0.5 a.u.—the IJV results are in very good agreement with the numerical solutions provided by TDSE method. In Fig. 2(b), as a result of the decrease in the frequency, the number of oscillations of the field inside the envelope is reduced to 3. Consequently, the structures of the electronic spectrum become less pronounced, tending to the collisional regime.

In Fig. 3 we investigate the momentum of the ejected

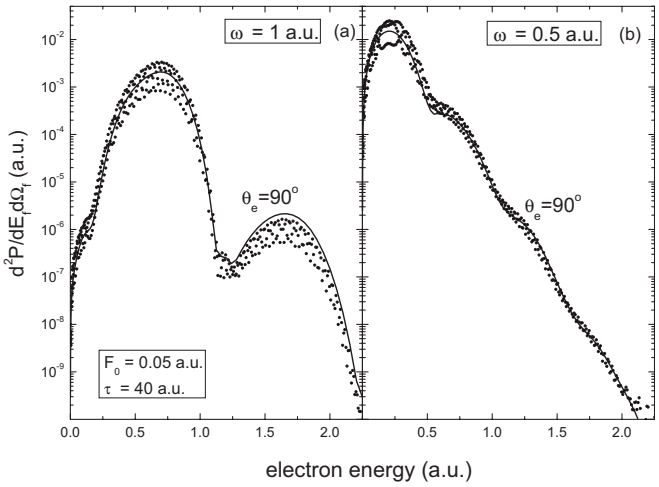

FIG. 2. Similar to Fig. 1 for the emission angle θ_e=90°. Laser field with F_0=0.05 a.u., τ=40 a.u., and frequency ω=(a) 1 and (b) 0.5 a.u.

electrons by plotting the two-dimensional electron distribution as a function of the component of the momentum perpendicular to the surface (k'_{fz}) on the horizontal axis and the component parallel to the surface (k_{fs}) on the vertical axis. The parameters of the pulse are the same as those in Fig. 1(b). The momentum distribution derived from the IJV approximation displays maxima as a function of k'_{fz}, which are related to the multiphoton peaks. The intensity of the maxima decreases steeply as the perpendicular momentum increases and the second maximum reaches a value two orders of magnitude lower than the former. In contrast with what happens in photoemission from atoms, in which electron momentum spectra present radial fanlike structures associated with the Coulomb potential of the residual target [21], the momentum spectrum of Fig. 3 shows nearly vertical stripes. This vertical pattern is related to the geometry of the problem, which imposes the conservation of the momentum parallel to the surface due to the noninclusion of corrugation effects in the surface plane.

In addition, we study the energy distribution of emitted electrons, dP/dE_f, which is derived by integrating the angu-

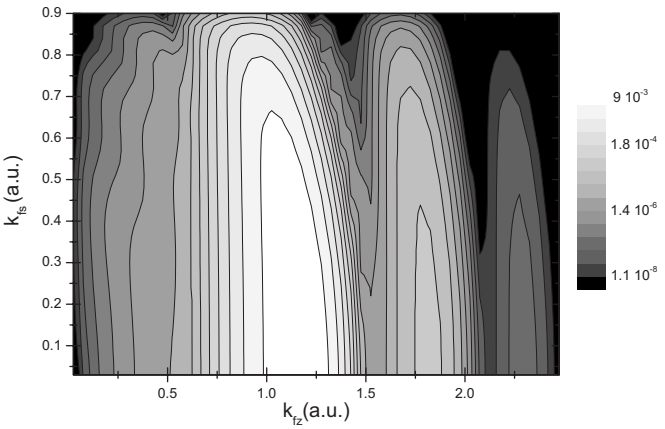

FIG. 3. Electron momentum distribution derived from IJV model for a laser pulse with F_0=0.1 a.u., ω=1 a.u., and τ=40 a.u.

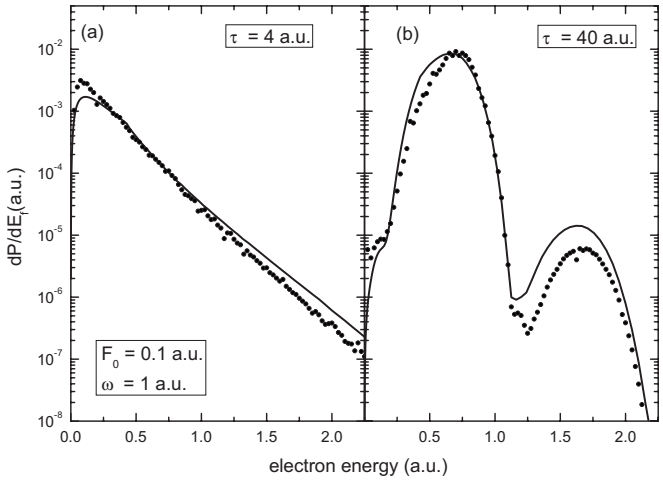

FIG. 4. Energy distribution of emitted electrons, as a function of the electron energy, for a laser field with $F_0=0.1$ a.u. and $\omega=1$ a.u. The duration of the pulse is $\tau=$(a) 4 and (b) 40 a.u. Solid line, IJV approach; full dots, TDSE results.

lar distribution $dP/dE_f d\Omega_f$ on the solid angle Ω_f, taking into account that only the semispace corresponding to the vacuum zone must be included in the integral. The single differential emission probability dP/dE_f is plotted in Fig. 4 for the same laser parameters as Fig. 1. When the field does not perform oscillations, as in Fig. 4(a), the probability decreases smoothly as a function of the electron energy and only displays a maximum at a very small electron velocity. For this case, results obtained with the IJV approach are in fair agreement with TDSE data but they show a slightly different slope as a function of the electron energy. In Fig. 4(b), as the duration of the pulse increases the spectrum displays the well-known above threshold ionization peaks. The energy distribution presents maxima at $E_f=0.65$ and 1.63 eV, which correspond to the absorption of one or two photons, where $E_f \simeq \langle E_i \rangle - U_p + n\omega$, with $\langle E_i \rangle = -0.32$ a.u. the initial

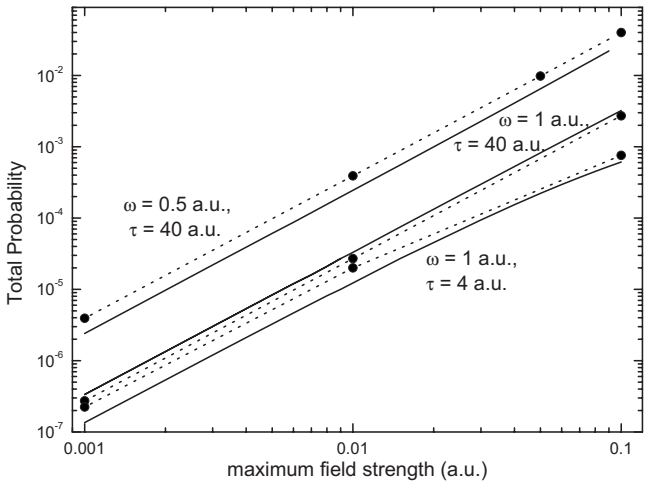

FIG. 5. Total emission probability as a function of the maximum field strength of the laser pulse. Three different sets of laser parameters are shown. Solid line, IJV model; full dots, TDSE results, with lines as a guide to the eyes.

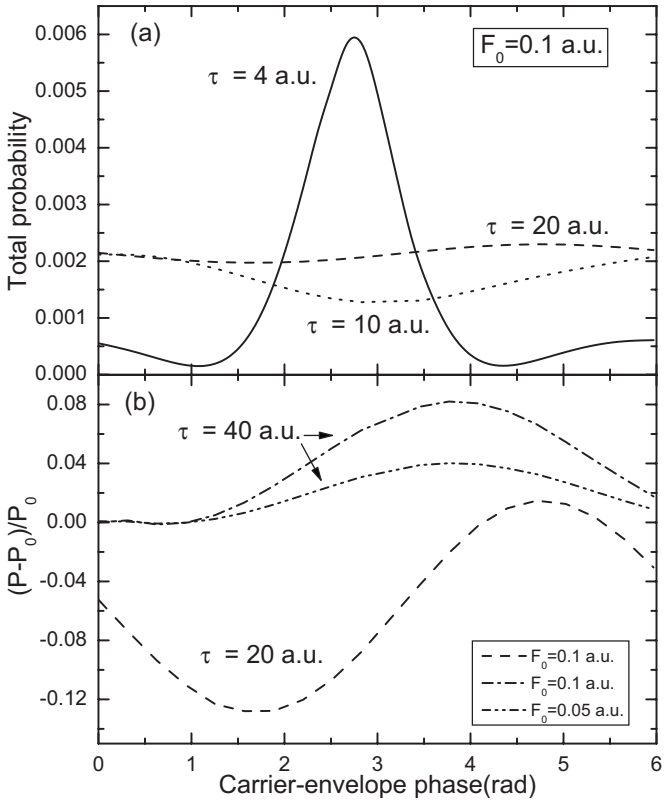

FIG. 6. Results obtained within the IJV model for (a) the probability P and (b) the relative probability ratio $R=(P-P_0)/P_0$, as a function of the carrier-envelope phase φ, with P (P_0) the total photoemission probability for a laser pulse with φ ($\varphi_0=-\omega\tau/2+\pi/2$). The laser frequency is $\omega=1$ a.u. Lines as defined in the figure.

mean energy, $U_p=F_0^2/(4\omega^2)$ the ponderomotive energy, and $n=1,2$ the number of photons. For oscillating fields we find a good agreement between the IJV and TDSE calculations, especially around the first peak, which provides the most important contribution to the total probability of electron emission. Remarkably, the dispersion of points observed in TDSE spectra of Figs. 1 and 2 completely disappears when the ejection angle is integrated to obtain the energy distribution. In Fig. 4, the TDSE values show a smooth behavior as a function of the electron energy, similar to that displayed for the IJV results.

B. Total emission probability

The dependence of the total emission probability on the intensity and the carrier-envelope phase of the laser pulse is here investigated. In Fig. 5 we show the total emission yield, which includes only external ionization, as a function of the maximum field strength F_0 for different durations and carrier frequencies of the pulse. In all the cases the emission process belongs to the weak field regime, with a Keldysh parameter $\gamma=\omega\sqrt{E_W}/F_0$ [22] greater than unity. As also observed in Ref. [5], the total emission probability P increases with F_0 following a power law, i.e., $P \sim F_0^x$. The exponent x varies only slightly with τ and displays a very weak dependence on ω, which might be a consequence of the absence of an in-

duced potential in our model. The TDSE results show a behavior qualitatively similar to the IJV values, both of them without signatures of saturation effects.

Finally, the IJV model is employed to study the dependence of the total probability of external electron emission on the carrier-envelope phase of the pulse. In Fig. 6(a) we plot the total emission probability P obtained with the IJV approach as a function of the phase φ for pulses with $\omega=1$ a.u. and different duration times. We find that, when the duration of the pulse is short enough to contain less than one oscillation inside the envelope, the probability P varies appreciably with φ, showing a maximum near π, as also found in Ref. [5]. But when τ increases—allowing the field to perform several oscillations—the carrier-envelope phase affects only the second maximum of the energy distribution dP/dE_f, while the first maximum stays invariable for different values of φ. Therefore, as P is mainly determined by the contribution of the first peak, for oscillating fields the total probability becomes almost independent of the carrier-envelope phase. In order to explore the φ dependence for longer pulses, in Fig. 6(b) we display the relative ratio $(P-P_0)/P_0$, where P_0 is the total probability corresponding to a symmetric pulse, with $\varphi=-\omega\tau/2+\pi/2$. For $\tau=20$ a.u. the relative variation with phase reaches up to 12% but it decreases as τ increases. The variation with φ also depends on the field strength F_0, becoming smaller for lower intensities of the field.

IV. CONCLUSIONS

In this work we have introduced the IJV approximation, which is a distorted-wave method based on the jellium model and the Volkov phase. The simple representation of the surface given by the jellium model allows us to include the proper asymptotic conditions in the final states, which are associated with electrons ejected toward the vacuum semispace. By comparing the proposed approach with values derived from the numerical solution of the corresponding TDSE, we conclude that the IJV theory provides reliable predictions of photoemission spectra for intense and short laser pulses. It is important to point out that the IJV approximation constitutes an inexpensive computational method. The total probability dependence on the intensity and carrier-envelope phase of the pulse is also investigated, finding a behavior qualitatively similar to that observed in Ref. [5].

ACKNOWLEDGMENTS

This work was done with the financial support of UBACyT, ANPCyT, and CONICET of Argentina. Computational work was carried out at the High-Performance Opteron Parallel Ensemble (HOPE) cluster at IAFE and at the National Energy Research Scientific Computing Center in Oakland, CA.

[1] D. B. Milošević, G. G. Paulus, D. Bauer, and W. Becker, J. Phys. B **39**, R203 (2006).
[2] A. Becker and F. H. M. Faisal, J. Phys. B **38**, R1 (2005).
[3] G. G. Paulus *et al.*, Nature (London) **414**, 182 (2001).
[4] G. G. Paulus, F. Lindner, H. Walther, A. Baltuska, E. Goulielmakis, M. Lezius, and F. Krausz, Phys. Rev. Lett. **91**, 253004 (2003).
[5] C. Lemell, X.-M. Tong, F. Krausz, and J. Burgdörfer, Phys. Rev. Lett. **90**, 076403 (2003).
[6] F. H. M. Faisal, J. Z. Kamiński, and E. Saczuk, Phys. Rev. A **72**, 023412 (2005).
[7] P. Dombi, F. Krausz, and G. Farkas, J. Mod. Opt. **53**, 163 (2006).
[8] D. M. Volkov, Z. Phys. **94**, 250 (1935).
[9] M. N. Faraggi, M. S. Gravielle, and V. M. Silkin, Phys. Rev. A **73**, 032901 (2006).
[10] M. S. Gravielle, Phys. Rev. A **58**, 4622 (1998).
[11] M. S. Gravielle, J. E. Miraglia, G. G. Otero, E. A. Sánchez, and O. Grizzi, Phys. Rev. A **69**, 042902 (2004).
[12] M. R. C. McDowell and J. P. Coleman, *Introduction to the Theory of Ion-Atom Collisions*, 1st ed. (North-Holland, Amsterdam, 1970).
[13] P. Macri, J. E. Miraglia, and M. S. Gravielle, J. Opt. Soc. Am. B **20**, 1801 (2003).
[14] H. R. Reiss, Phys. Rev. A **22**, 1786 (1980).
[15] O. Smirnova, M. Spanner, and M. Ivanov, J. Phys. B **39**, S307 (2006).
[16] G. L. Yudin, S. Patchkovskii, P. B. Corkum, and A. D. Bandrauk, J. Phys. B **40**, F93 (2007).
[17] D. P. Dewangan and J. Eichler, Phys. Rep. **247**, 59 (1997).
[18] W. H. Press, S. A. Teukolsky, W. T. Vetterling, and B. P. Flannery, *Numerical Recipes* (Cambridge University Press, New York, 1992).
[19] M. S. Pindzola, F. Robicheaux, J. Colgan, D. M. Mitnik, D. C. Griffin, and D. R. Schultz, in *Photonic, Electronic, and Atomic Collisions: ICPEAC XXII*, edited by J. Burgdörfer, J. S. Cohen, S. Datz, and C. R. Vane (Rinton Press, Princeton, NJ, 2002), p. 483.
[20] M. S. Pindzola, F. Robicheaux, S. D. Loch, J. C. Berengut, T. Topcu, J. Colgan, M. Foster, D. C. Griffin, C. P. Ballance, D. R. Schultz, T. Minami, N. R. Badnell, M. C. Witthoeft, D. R. Plante, D. M. Mitnik, J. A. Ludlow, and U. Kleiman, J. Phys. B **40**, R39 (2007).
[21] D. G. Arbó, S. Yoshida, E. Persson, K. I. Dimitriou, and J. Burgdörfer, Phys. Rev. Lett. **96**, 143003 (2006).
[22] L. V. Keldysh, Sov. Phys. JETP **20**, 1307 (1965).